J. Fluid Mech. (2013), *vol.* 726, *pp.* 137–159.
doi:10.1017/jfm.2013.175

Solitary waves in turbulent open-channel flow

Wilhelm Schneider†

Institute of Fluid Mechanics and Heat Transfer, Vienna University of Technology, 1040 Vienna, Austria

(Received 12 December 2012; revised 18 February 2013; accepted 27 March 2013;
first published online 30 May 2013)

Two-dimensional turbulent free-surface flow is considered. The ensemble-averaged flow quantities may depend on time. The slope of the plane bottom of the channel is assumed to be small. The roughness of the bottom is allowed to vary with the space coordinate, leading to small variations in the bottom friction coefficient. An asymptotic analysis, which is free of turbulence modelling, is performed for large Reynolds numbers and Froude numbers close to the critical value 1. As a result, an extended Korteweg–deVries (KdV) equation for the surface elevation is obtained. Other flow quantities, such as pressure, flow velocity components, and bottom shear stress, are expressed in terms of the surface elevation. The steady-state version of the extended KdV equation has eigensolutions that describe stationary solitary waves. Time-dependent solutions of the extended KdV equation provide a means for discriminating between stable and unstable stationary solitary waves. Solutions of initial value problems show that there are transient solutions that approach asymptotically the stable stationary solitary wave, whereas other transient solutions decay asymptotically with increasing time.

Key words: solitary waves, turbulent flows, free-surface flows

1. Introduction

The behaviour of solitary waves in turbulent open-channel flow is studied in the present work, with the particular aim of investigating whether solitary waves may exist in steady flow, i.e. as stationary solitary waves. On the basis of momentum considerations it may be expected that stationary solitary waves cannot exist in turbulent open-channel flow over plane bottoms with constant roughness. The present results will confirm that presumption, cf. § 4.1. Thus the following analysis will allow for varying bottom roughness. The law of momentum can then be satisfied by compensating the combined effects of the additional weight and the velocity decrease in the solitary wave by a suitable increase of the friction coefficient.

Various *ad-hoc* approximations have been commonly applied, often quite successfully, in open-channel hydraulics, cf. the classical work by Hager & Hutter (1984), or the more recent examples due to Castro-Orgaz & Chanson (2011), Mohamed (2010), Castro-Orgaz & Hager (2011), and Bose, Castro-Orgaz & Dey (2012). Furthermore, a variety of models for bottom friction has been applied, cf. Miles (1983*a*,*b*), Caputo & Stepanyants (2003), Grimshaw, Pelinovsky & Talipova (2003), El, Grimshaw & Kamchatkov (2007), and Castro-Orgaz (2010). In contrast,

† Email address for correspondence: wilhelm.schneider@tuwien.ac.at

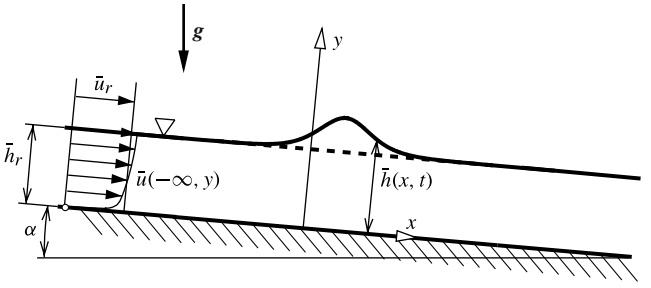

FIGURE 1. A solitary wave in turbulent open-channel flow.

the present analysis is based on a rigorous asymptotic expansion for large Reynolds numbers and Froude numbers close to the critical value 1.

The main result of the asymptotic analysis will be an extended Korteweg–deVries (KdV) equation. Special cases of the present result have been obtained previously. For constant bottom roughness, the steady-state version of the extended KdV equation was derived by Grillhofer & Schneider (2003) in an analysis of the undular hydraulic jump. Later the analysis was extended to account for the possibility of non-developed flow far upstream, leading to the steady-state version of an extended KdV equation with a constant 'forcing' term, cf. Schneider (2005), Jurisits, Schneider & Bae (2007), and Jurisits & Schneider (2012). In addition, a variable forcing term in the steady-state version of an extended KdV equation was obtained under the condition that the surface pressure is subject to a space-dependent perturbation (Schneider, Jurisits & Bae 2010). On the basis of that equation, an asymptotic iteration procedure was developed for the numerical solution of the full equations of motion of near-critical free-surface flows, and the method was applied to the undular jump. Finally, it should be mentioned that an extended KdV equation of the present type, yet without the forcing term, has already been obtained as the result of an asymptotic analysis of undular hydraulic bores (Kang 2009).

Since the KdV equation and its extensions serve to model a large variety of physical processes, cf. Newell (1985), Christov & Velarde (1995), Scott (2003) and the references given therein, there are also a large number of papers dealing with the solutions or methods of solution. In the present context the monographs by DeKerf (1988), Johnson (1997) or Scott (2003), as well as the survey articles by Grimshaw (2005, 2007, 2010) are of particular interest. Equations similar to the present one have been considered by Ott & Sudan (1970), Leibovich & Randall (1971, 1973), Knickerbocker & Newell (1980), Caputo & Stepanyants (2003), Grimshaw, Zhang & Chow (2007), Chardard *et al.* (2011) and Abd-el-Malek & Helal (2011), among others.

2. Governing equations

2.1. *Reference quantities and non-dimensional variables*

Two-dimensional turbulent free-surface flow over a plane bottom with small, constant slope α is considered, see figure 1. Surface tension will be neglected. Ensemble-averaged quantities will be denoted by an overbar, fluctuations around the average by a prime. The main goal of the analysis is to determine the averaged surface height, $\bar{h}$, as a function of time and space coordinates. A Cartesian coordinate system is chosen such that the x-axis is in the bottom plane, while the y-axis points upwards. The flow velocity components in the (x, y) coordinate system are u and v, respectively. The flow

far upstream is assumed to be in a steady state and fully developed, i.e. $\bar{u} = \bar{u}(-\infty, y)$, $\bar{v} \equiv 0$, and $\bar{h} = \bar{h}_r = \text{const}$ as $x \to -\infty$. Note that in the present paper the term 'fully developed' implies mechanical equilibrium of gravity and bottom-friction forces, in accord with the definition commonly used in theoretical fluid mechanics. Some experimentalists, however, use a weaker definition, i.e. the flow is said to be fully developed when the edge of the boundary layer that originates at the bottom reaches the surface.

For introducing non-dimensional variables, the flow far upstream is chosen as a reference state, which is denoted by the subscript r. Thus $\bar{h}_r$ serves as reference length, while the volumetric mean velocity $\bar{u}_r$, $\bar{u}_r = \dot{V}/\bar{h}_r$, is chosen as the reference velocity, with $\dot{V}$ being the constant volume flow rate per unit width of the channel. As has been shown previously for the related problem of undular jumps (Grillhofer & Schneider 2003), choosing the volumetric mean velocity as the reference velocity is essential for keeping the analysis free of turbulence modelling. Concerning further dimensionless quantities, the pressure is referred to the hydrostatic pressure at the bottom of the channel far upstream, i.e. $g\rho\bar{h}_r$, where g is the acceleration due to gravity and ρ is the constant density of the fluid. The Reynolds stresses are referred to the wall shear stress far upstream, which may be written as $\rho u_{\tau r}^2$, where $u_{\tau r}$ is the reference value of the friction velocity, u_τ. Since the wall shear stress balances the tangential component of the gravity force in fully developed flow, $u_{\tau r}$ is given by

$$u_{\tau r} = \sqrt{g\alpha\bar{h}_r}. \tag{2.1}$$

It is well known that inviscid solitary waves with amplitudes of the order of ε, with $\varepsilon \ll 1$, have wavelengths of the order of $1/\sqrt{\varepsilon}$ in terms of the depth of the fluid layer. Anticipating that the same relationship for the orders of magnitude will also hold in the case of turbulent flows at large Reynolds numbers, a small parameter δ is introduced as

$$\delta = 3\sqrt{\varepsilon} \tag{2.2}$$

for the purpose of stretching the longitudinal coordinate, x. The coefficient 3 has been chosen merely in the interest of simplifying the final equation.

With regard to the time t it would be straightforward to introduce $\bar{h}_r/\bar{u}_r$ or, in view of the large wavelengths, $\delta^{-1}\bar{h}_r/\bar{u}_r$ as a reference time. But neither of those reference times would characterize the time scale of the slow decay of the solitary wave due to the effects of turbulence at large Reynolds numbers. Thus we introduce another small parameter, σ, with the purpose of stretching the time such that the time-derivative term in the non-dimensional final equation is of the same order of magnitude as the terms containing space derivatives. As the analysis will show, this aim can be achieved with the choice

$$\sigma = (9/2)\,\varepsilon^{3/2}, \tag{2.3}$$

where the coefficient $9/2$ serves to simplify the final equation.

Non-dimensional variables are then introduced as follows:

$$X = \delta\, x/\bar{h}_r, \quad Y = y/\bar{h}_r, \quad T = \sigma\,(\bar{u}_r/\bar{h}_r)\,t, \quad \bar{H} = \bar{h}/\bar{h}_r, \quad \bar{U} = \bar{u}/\bar{u}_r, \quad \bar{V} = \delta^{-1}\bar{v}/\bar{u}_r, \tag{2.4a}$$

$$\bar{P} = \bar{p}/g\rho\bar{h}_r, \quad \overline{U'^2} = \overline{u'^2}/u_{\tau r}^2, \quad \overline{U'V'} = \overline{u'v'}/u_{\tau r}^2, \quad \overline{V'^2} = \overline{v'^2}/u_{\tau r}^2, \quad U_\tau = u_\tau/u_{\tau r}. \tag{2.4b}$$

Note that $\bar{H}$ and U_τ are unknown functions of X and T, while the other flow quantities depend also on Y.

Concerning viscosity effects, very large Reynolds numbers will be considered. It is common practice in the asymptotic analysis of turbulent flow to define the Reynolds number in terms of the reference friction velocity, i.e.

$$Re_\tau = u_{\tau r}\bar{h}_r/\nu = (g\alpha)^{1/2}\bar{h}_r^{3/2}\nu^{-1}, \tag{2.5}$$

where ν is the kinematic viscosity. In the limit of large Reynolds numbers the flow field is composed of two layers, i.e. the defect layer and the thin viscous wall layer at the bottom. Concerning the latter, a universal solution is known to exist for steady flow, cf. Gersten & Herwig (1992), Kluwick (1998), or Schlichting & Gersten (2000). For the present unsteady flow, the estimate given in appendix A shows that the time-derivative term in the equations of motion of the viscous wall layer is of $O(\varepsilon\delta\, Re_\tau^{-1}\ln Re_\tau) \to 0$ as $\varepsilon \to 0$ and $Re_\tau \to \infty$. Thus the universal wall layer solution is applicable to the present case, and it is sufficient to consider only the defect layer in what follows.

2.2. *Equations of motion*

In terms of the present non-dimensional variables, the continuity equation reads

$$\bar{U}_X + \bar{V}_Y = 0. \tag{2.6}$$

Here, and in what follows if convenient, derivatives are indicated by subscripts.

Since viscous stresses are negligible in the defect layer, whereas the Reynolds stresses are of essential importance, the momentum equations for the ensemble-averaged quantities become

$$Fr^2\left(\frac{3\varepsilon}{2}\frac{\partial\bar{U}}{\partial T} + \bar{U}\frac{\partial\bar{U}}{\partial X} + \bar{V}\frac{\partial\bar{U}}{\partial Y}\right) = -\frac{\partial\bar{P}}{\partial X} + \frac{\alpha}{\delta} - \frac{\alpha}{\delta}\left(\delta\frac{\partial\overline{U'^2}}{\partial X} + \frac{\partial\overline{U'V'}}{\partial Y}\right), \tag{2.7a}$$

$$\delta^2 Fr^2\left(\frac{3\varepsilon}{2}\frac{\partial\bar{V}}{\partial T} + \bar{U}\frac{\partial\bar{V}}{\partial X} + \bar{V}\frac{\partial\bar{V}}{\partial Y}\right) = -\frac{\partial\bar{P}}{\partial Y} - 1 - \alpha\left(\delta\frac{\partial\overline{U'V'}}{\partial X} + \frac{\partial\overline{V'^2}}{\partial Y}\right), \tag{2.7b}$$

with the Froude number

$$Fr = \bar{u}_r/\sqrt{g\bar{h}_r}. \tag{2.8}$$

Note that the momentum equations would contain additional terms if time-averaged, instead of ensemble-averaged, quantities were used, see Schlichting & Gersten (2000), p. 644.

2.3. *Boundary and matching conditions*

The system of basic equations (2.6), (2.7*a*) and (2.7*b*) is to be solved subject to appropriate boundary conditions. Since the viscous wall layer is very thin, the normal velocity component in the defect layer has to satisfy the conventional boundary condition at the bottom, i.e.

$$\bar{V}(X, 0, T) = 0. \tag{2.9}$$

Matching the defect-layer solution to the wall-layer solution will be accomplished by making use of the well-known logarithmic 'overlap law', commonly also known as

the 'law of the wall'. Following Schlichting & Gersten (2000), p. 534, the following expression for the non-dimensional surface velocity is obtained:

$$\bar{U}(X,\bar{H},T)=\sqrt{\alpha}Fr^{-1}U_\tau[(1/\kappa)\ln(Re_\tau U_\tau\bar{H})+C^+(X)+\bar{C}(X,T)], \tag{2.10}$$

where κ is von Kármán's constant, commonly taken to be 0.41, while

$$\bar{C}(X,T)=\int_0^{\bar{H}}\left(\frac{Fr}{\sqrt{\alpha}U_\tau}\frac{\partial\bar{U}}{\partial Y}-\frac{1}{\kappa Y}\right)\mathrm{d}Y. \tag{2.11}$$

C^+ is an empirical function of the non-dimensional roughness, k_s^+, with $k_s^+=k_su_\tau/\nu=\sqrt{g\alpha\bar{h}_r}k_sU_\tau/\nu$, where k_s is the sand roughness height, cf. Schlichting & Gersten (2000), pp. 526–528. As an alternative to the sand roughness, the non-dimensional technical roughness may be used, cf. also Schlichting & Gersten (2000), pp. 529–532. In the present analysis, the roughness is allowed to vary with X, leading to $C^+=C^+(X)$. For a hydraulically smooth bottom ($k_s^+\ll 1$), the generally accepted value of C^+ is $C^+=5.0$, while in the limiting case of a fully rough bottom ($k_s^+\to\infty$) C^+ varies according to the relationship $C^+=(1/\kappa)\ln(1/k_s^+)+8.0$.

A further matching condition is required for the Reynolds shear stress. Written in non-dimensional variables it becomes

$$-\overline{U'V'}=U_\tau^2\quad\text{as } Y\to 0. \tag{2.12}$$

At the free surface, kinematic and dynamic boundary conditions have to be satisfied. The kinematic boundary condition is prescribed in the conventional form, i.e.

$$\bar{V}(X,\bar{H})=\tfrac{3}{2}\varepsilon\bar{H}_T+\bar{U}(X,\bar{H})\bar{H}_X. \tag{2.13}$$

Equation (2.13) defines the averaged surface such as to ensure that an element of the ensemble-averaged surface $Y=\bar{H}(X,T)$ remains in the surface as it moves with the ensemble-averaged velocity $(\bar{U},\bar{V})$. With respect to the dynamic boundary conditions, which express continuity of stresses at the free surface, we follow the conventional approach, cf. Rodi (1993). With surface tension and viscous stresses being neglected, but Reynolds stresses being taken into account, the dynamic boundary conditions with respect to the X- and Y-directions, respectively, then become

$$-[\bar{P}(X,\bar{H},T)+\alpha\overline{U'^2}(X,\bar{H},T)]\sin\vartheta+\alpha\overline{U'V'}(X,\bar{H},T)\cos\vartheta=0, \tag{2.14a}$$

$$[\bar{P}(X,\bar{H},T)+\alpha\overline{V'^2}(X,\bar{H},T)]\cos\vartheta-\alpha\overline{U'V'}(X,\bar{H},T)\sin\vartheta=0, \tag{2.14b}$$

where ϑ is the inclination angle of the averaged free surface with respect to the horizontal, i.e. $\tan\vartheta=\delta\bar{H}_X$. The application of 'conventional' boundary conditions at the free surface, i.e. (essentially) vanishing Reynolds shear stress at the surface, has been justified, among others, by Komori *et al.* (1993) and Handler *et al.* (1993). It is in agreement with measurements due to Nezu & Rodi (1986) and Lennon & Hill (2006), though (rather small) deviations have also been detected, see Brocchini & Peregrine (1998) and Svendsen *et al.* (2000).

3. Derivation of an extended KdV equation by asymptotic analysis

3.1. *Asymptotic expansions*

Solitary waves with small amplitudes of the order ε are known to move in an inviscid, quiescent fluid with a velocity that corresponds to a slightly supercritical Froude number, i.e. $Fr=1+O(\varepsilon)$. Thus the following relationship between the Froude number

and the small parameter ε is postulated, introducing a coefficient 3/2 that serves for later convenience:

$$Fr = 1 + \tfrac{3}{2}\varepsilon \quad (0 < \varepsilon \ll 1). \tag{3.1}$$

So far, two small parameters, i.e. ε and α, have been introduced. Their relative size is now chosen as follows. Since it is one of the aims of the present work to determine how turbulence affects the existence and propagation of solitary waves, it is necessary, on the one hand, that the leading terms due to turbulence, though small, are retained in the analysis. On the other hand, it is intended to keep the analysis free of turbulence modelling by appropriately limiting the magnitude of the Reynolds stresses. These two requirements turn out to be satisfied if α is of the order of ε^2. Therefore the coupling parameter

$$A = \alpha/\varepsilon^2 \tag{3.2}$$

is introduced, and in performing an asymptotic expansion for small values of ε it is assumed that $A = O(1)$.

The dependent variables are now expanded in terms of powers of ε, e.g.

$$\bar{H}(X, T) = H_0 + \varepsilon\, H_1(X, T) + \varepsilon^2 H_2(X, T) + o(\varepsilon^2), \tag{3.3}$$

$$\bar{U}(X, Y, T) = U_0(Y) + \varepsilon\, U_1(X, Y, T) + \varepsilon^2 U_2(X, Y, T) + o(\varepsilon^2), \tag{3.4}$$

$$\overline{U'V'}(X, Y, T) = (\overline{U'V'})_0(Y) + \varepsilon\, (\overline{U'V'})_1(X, Y, T) + \varepsilon^2 (\overline{U'V'})_2(X, Y, T) + o(\varepsilon^2). \tag{3.5}$$

To keep the analysis free of turbulence modelling, several important points have to be observed. First, the volumetric mean velocity of the fully developed flow far upstream has to be taken as the reference velocity, as already noted above. Secondly, the surface height of the fully developed flow, i.e. the reference height $\bar{h}_r$, ought to be known for given values of bottom slope, α, and volume flow rate, $\dot{V}$. This implies that the friction coefficient of the channel with unperturbed bottom roughness, c_{fr}, is known, as the force balance gives $\bar{h}_r = (c_{fr}\dot{V}^2/2g\alpha)^{1/3}$. Thirdly, the non-dimensional 'velocity defect' $\Delta U = \Delta U(Y)$ will be introduced such that the local value of $\bar{U}$ in the fully developed flow far upstream differs from its volumetric mean, i.e. 1, by the amount $\sqrt{\alpha}\,\Delta U$. This quantity could be considered as known from experiments (e.g. Nezu & Rodi 1986), but it will turn out that the final result does not contain it. In addition, the perturbation of the defect velocity profile, which leads to a perturbation of $\bar{C}$ as defined by (2.11), will appear only in terms of higher-order than presently considered. Finally, it is of importance to apply the logarithmic 'law of the wall' ('overlap law') in a suitable form, such as (2.10). On that basis, the asymptotic analysis, which requires some subtle manipulations, can be performed as follows.

3.2. *First-order equations*

With the basic state given by the simple relations

$$H_0 = 1, \quad U_0 = 1, \quad V_0 = 0, \quad P_0 = 1 - Y, \quad (\overline{U'V'})_0 = Y - 1, \tag{3.6}$$

the expansion of the continuity equation (2.6) leads to $U_{1X} + V_{1Y} = 0$, which can be integrated to obtain

$$V_1 = -\int_0^Y U_{1X}\,\mathrm{d}Y, \tag{3.7}$$

where the boundary condition at the bottom, (2.9), has already been satisfied.

Before expanding the momentum equations (2.7*a*) and (2.7*b*) for small values of ε, the small parameters δ and α are expressed in terms of ε according to (2.2) and (3.2), respectively. Expanding then (2.7*b*) gives $P_{1Y} \equiv 0$, i.e.

$$P_1 = P_1(X, T). \tag{3.8}$$

Then expanding (2.7*a*), one obtains $U_{1X} = -P_{1X}$. This can also be integrated. The free function of integration is determined from relations characterizing the fully developed flow far upstream, i.e. $P_1 \equiv 0$, $U_1 = \sqrt{A}\,\Delta U(Y)$ as $X \to -\infty$. $\Delta U(Y)$ is the non-dimensional velocity defect, which is introduced as described in the last paragraph of the preceding section. Therewith one obtains the relation

$$U_1(X, Y, T) = -P_1(X, T) + \sqrt{A}\,\Delta U(Y). \tag{3.9}$$

Next, the following relations follow from the dynamic boundary conditions (2.14*b*) and (2.14*a*), in this order:

$$P_1(X, T) = H_1(X, T), \tag{3.10}$$

$$(\overline{U'V'})_1(X, 1, T) = -H_1(X, T). \tag{3.11}$$

Taking (3.9) and (3.10) into account, the integration in (3.7) can be performed, with the result

$$V_1 = Y H_{1X}. \tag{3.12}$$

Finally, the logarithmic law (2.10) is expanded together with (2.11). Concerning the expansion of the latter equation it suffices to formally write $\bar{C}(X, T) = \bar{C}_r + \varepsilon \bar{C}_1(X, T)$, where $\bar{C}_r$ denotes the value of $\bar{C}$ in the reference state, i.e. for the fully developed flow. Using (2.5) and (2.12), one obtains the following relation:

$$\begin{aligned} 1 + \varepsilon U_1(X, 1, T) + \cdots = {} & \frac{\sqrt{\alpha}}{Fr}\left(\frac{1}{\kappa}\ln\frac{\sqrt{g\alpha\bar{h}_r^3}}{\nu} + C^+ + \bar{C}_r\right) \\ & + \frac{\varepsilon\sqrt{\alpha}}{Fr}\left[-\frac{1}{2}(\overline{U'V'})_1(X, 0, T)\left(\frac{1}{\kappa}\ln\frac{\sqrt{g\alpha\bar{h}_r^3}}{\nu} + C^+ + \bar{C}_r + \frac{1}{\kappa}\right) + \frac{H_1}{\kappa} + \bar{C}_1\right] + \cdots. \end{aligned} \tag{3.13}$$

Far upstream, the velocity perturbation is given by the velocity defect of the fully developed flow, the perturbation of the Reynolds shear stress vanishes, and the roughness is equal to the constant reference value, i.e.

$$X \to -\infty: \quad U_1 = \sqrt{A}\,\Delta U(Y); \quad (\overline{U'V'})_1 \equiv 0; \quad C^+ = C_r^+; \quad \bar{C}_1 = 0. \tag{3.14}$$

The value of C^+ in the reference state, i.e. far upstream, is denoted by C_r^+ and assumed to be constant. The bottom far upstream may, or may not, be hydraulically smooth. In the former case, the value $C_r^+ = 5.0$ is appropriate, as mentioned above, cf. the first paragraph following (2.11).

Comparing (3.14) with (3.13) shows that the logarithmic terms in the latter equation may be substituted according to the relation

$$\frac{\sqrt{\alpha}}{Fr}\left(\frac{1}{\kappa}\ln\frac{\sqrt{g\alpha\bar{h}_r^3}}{\nu} + C_r^+ + \bar{C}_r\right) = 1 + \varepsilon\sqrt{A}\,\Delta U(1), \tag{3.15}$$

to obtain

$$(\overline{U'V'})_1(X,0,T) = 2[H_1 + \sqrt{A}(C^+ - C_r^+)], \tag{3.16}$$

where Fr has been replaced by 1 at leading order, $\sqrt{A}\,\Delta U(1)$ has been eliminated with the help of (3.9) and (3.10), and the assumption has been made that $(C^+ - C_r^+) = O(1)$, with $(C^+ - C_r^+) \to 0$ as $X \to \pm\infty$. Note that $Y = 0$ refers to the channel bottom in terms of defect-layer coordinates, i.e. $-(\overline{U'V'})_1(X,0,T)$ is equal to the first-order perturbation of the bottom shear stress, cf. (2.12).

With (3.9)–(3.12) and (3.16), the results of the expansion up to first order are complete. Obviously, either $H_1(X,T)$ or $P(X,T)$ remain free in the framework of the first-order equations. Thus, the second-order equations have to be inspected for solvability.

3.3. *An extended KdV equation as solvability condition of the second-order equations*

Expanding, first, the momentum equation (2.7*b*) up to second order, making use of the first-order results of § 3.2, integrating with respect to Y and determining a free function of integration from the dynamic boundary condition (2.14*b*) at second order, gives

$$P_2 - H_2 = \tfrac{9}{2}H_{1XX}\left(1 - Y^2\right) - A\left(\overline{V'^2}\right)_0, \tag{3.17}$$

where the last term on the right-hand side of the equation is a function of Y only. Secondly, the momentum equation (2.7*a*) is also expanded up to second order, retaining the term of the order $\beta\varepsilon^2$, where $\beta = A\sqrt{\varepsilon}/3$, to obtain

$$U_{2X} + P_{2X} = -\tfrac{3}{2}U_{1T} - U_1U_{1X} - V_1U_{1Y} - 3U_{1X} - \beta\left(\overline{U'V'}\right)_{1Y}. \tag{3.18}$$

Concerning the order of magnitude of the term containing the coefficient β see the discussion following (3.24). U_{2X} may be replaced by $-V_{2Y}$ according to the expanded version of the continuity equation (2.6), and, furthermore, P_2 may be eliminated using (3.17). The equation hence obtained can then be integrated with respect to Y, accounting for the boundary condition at the bottom, (2.9). Introducing, once more, the first-order results and observing that, by definition,

$$\int_0^1 \Delta U\,\mathrm{d}Y = 0, \qquad \int_0^1 Y\,(\Delta U)_Y\,\mathrm{d}Y = \Delta U(1), \tag{3.19}$$

one obtains the following relation:

$$\begin{aligned} V_2(X,1,T) - H_{2X} = {} & -\tfrac{3}{2}H_{1T} + 3H_{1XXX} - \left[3 - H_1 - \sqrt{A}\,\Delta U(1)\right]H_{1X} \\ & - \beta\left[3H_1 + 2\sqrt{A}(C^+ - C_r^+)\right]. \end{aligned} \tag{3.20}$$

On the other hand, the second-order kinematic boundary condition, which follows from (2.13) upon expanding, gives

$$V_2(X,1,T) - H_{2X} = \tfrac{3}{2}H_{1T} - \left[2H_1 - \sqrt{A}\,\Delta U(1)\right]H_{1X}. \tag{3.21}$$

Equations (3.20) and (3.21) are compatible if H_1 satisfies the equation

$$H_{1XXX} + (H_1 - 1)H_{1X} - H_{1T} = \beta[H_1 - \Gamma(X)], \tag{3.22}$$

with

$$\beta = \tfrac{1}{3}A\sqrt{\varepsilon} = \tfrac{1}{3}\alpha\varepsilon^{-3/2} \tag{3.23}$$

and

$$\Gamma(X) = \tfrac{2}{3}\sqrt{A}[C_r^+ - C^+(X)], \tag{3.24}$$

where $\sqrt{A} = \sqrt{\alpha}/\varepsilon$ according to (3.2). Note that $\Delta U(1)$ has cancelled, so that knowledge of the velocity defect is not required.

Equation (3.22), which describes the evolution of the surface elevation in a first approximation, can be recognized as an extended KdV equation. The 'forcing term' $\Gamma(X)$ vanishes far upstream in accordance with previous assumptions, i.e. $\Gamma(X) = 0$ as $X \to -\infty$. In the present study the case $\Gamma(X) > 0$ will be of interest. In general, positive values of Γ can be obtained with locally enhanced values of roughness, but small regular roughness elements are an exception, cf. Schlichting & Gersten (2000), pp. 528 and 529.

According to (3.23) and (2.1) the parameter β is proportional to the square of the reference friction velocity, $u_{\tau r}$. This indicates that β characterizes dissipation. The limiting case $\beta = 0$ corresponds to inviscid flow, for which (3.22) reduces to the classical KdV equation.

On the basis of the assumption that $A = O(1)$, it follows from (3.23) that $\beta = O(\varepsilon^{1/2})$, i.e. half an order of magnitude smaller than the other terms in (3.22), which are of order one. This is unavoidable if conventional variables are retained in the asymptotic analysis. In the notion of Van Dyke (1975), the present asymptotic expansion is a 'method of composite equations', leading to a 'uniformly valid differential equation'. For a famous example of uniformly valid differential equations, Van Dyke (1975) refers to Oseen's equation for viscous flow at very small Reynolds numbers. If formal Poincaré expansions were preferred, singular perturbation methods (e.g. the method of multiple scales) would have to be applied. For steady flow, such a rather elaborate approach has been pursued by Steinrück, Schneider & Grillhofer (2003) for the special case $\Gamma \equiv 0$, and by Steinrück (2010) for the more general case $\Gamma = \text{const} \neq 0$. The latter work also contains a proof of the uniform validity of the steady-state version of (3.22).

It might be of interest to observe that (3.22) does not resemble the corresponding equation for laminar flow, which is a Korteweg–deVries–Burgers equation, with dissipation effects described by a second space derivative of the surface elevation (Johnson 1972, 1997; Whitham 1999, pp. 482–484; cf. also the triple-deck analysis by Kluwick *et al.* 2010). Instead, the dissipation term is a linear function of the surface elevation itself, corresponding to what Pelinovsky, Stepanyants & Talipova (1993) and Caputo & Stepanyants (2003) call the 'Rayleigh model of dissipation'.

Concerning other dissipation models, it may be observed that there is a formal similarity between (3.22) and the left-hand side of equation (1) of El *et al.* (2007), though with different meanings of the coefficients. On the right-hand side of the latter equation there is a quadratic term that is attributed to 'Chezy's model' of bottom friction in a turbulent boundary layer. However, Grillhofer (2002) has already shown that adding a quadratic friction term to the Euler equations for steady flow, and performing an asymptotic expansion for Froude numbers close to the critical value 1, leads to the steady-state version of (3.22) for $\Gamma = 0$, i.e. to a linear term representing weak dissipation. Thus, Grillhofer's result casts doubts on the applicability of Chezy's model to describe stationary solitary waves in turbulent open-channel flow.

It is also remarkable that (3.22) is free of non-local terms, in contrast to results obtained by Dutykh & Dias (2007) and Dutykh (2009). However, the analysis due to Dutykh & Dias (2007) and to Dutykh (2009) is based on assumptions that differ from the present ones. In particular, according to Dutykh & Dias (2007) and Dutykh (2009) the main source of dissipation is a viscous boundary layer whose thickness is of the order of $1/\sqrt{Re}$, where Re is a Reynolds number defined in terms of a constant viscosity as in laminar flow. That is in contrast to the scaling parameters of the present analysis of turbulent flow, where the viscous wall layer has a thickness of the order of $1/Re_\tau$, while an apparent viscosity, if introduced, would not be constant but vary across the layer. Obviously, those differences between the two types of analyses are responsible for the lack of non-local terms in (3.22).

When H_1 has been determined as a solution of (3.22), the first-order perturbations of pressure, P_1, normal velocity, V_1, and bottom shear stress, $-(\overline{U'V'})_1(X,0,T)$, follow from (3.10), (3.12), and (3.16), respectively. Furthermore, as the cross-sectional average of the velocity defect vanishes according to the definition of the reference velocity, it follows from (3.9) together with (3.10) that the cross-sectional average (i.e. the volumetric mean) of the tangential velocity perturbation equals $-H_1$, which expresses conservation of mass in a quasi-steady one-dimensional approximation. Defining, as usual, the bottom friction coefficient, c_f, in terms of the volumetric mean of the velocity and making use of (3.16), the perturbation of the friction coefficient due to the increased roughness can be expressed as follows:

$$(c_f - c_{fr})/c_{fr} = 2\sqrt{\alpha}(C_r^+ - C^+) = 3\varepsilon\, \Gamma(X), \tag{3.25}$$

where c_{fr} is the friction coefficient in the reference state, i.e. far upstream. It is remarkable that all these results have been obtained without recourse to turbulence modelling.

The partial differential equation (3.22) is to be solved subject to appropriate boundary and initial conditions. For investigating how turbulence affects the existence and evolution of solitary waves, the asymptotic decay of the perturbations far downstream and far upstream provides the following boundary conditions:

$$H_1 \to 0 \quad \text{as } X \to \pm\infty. \tag{3.26}$$

The initial conditions will depend on the particular problem to be considered.

4. Stationary solitary waves

4.1. *Steady-state version of the extended KdV equation*

In case of steady flow, the extended KdV equation (3.22) reduces to the ordinary differential equation

$$H_{1XXX} + (H_1 - 1)H_{1X} = \beta[H_1 - \Gamma(X)]. \tag{4.1}$$

Subscripts are retained to indicate derivatives, though H_1 is, of course, a function of X only in the steady-flow case.

For later convenience, (4.1) may be transformed, following Steinrück (2005), into the following set of first-order equations:

$$R_X = \beta[H_1 - \Gamma(X)]; \tag{4.2a}$$

$$S_X = -\beta H_1[H_1 - \Gamma(X)]; \tag{4.2b}$$

$$3(H_{1X})^2 + H_1^3 - 3H_1^2 - 6RH_1 = 6S. \tag{4.2c}$$

An equation of the type of (4.1), but without the term proportional to H_1, was considered by Dias & Vanden-Broeck (2002, 2004) and by Binder, Vanden-Broek & Dias (2005). Equations similar to (4.1) have also been studied as the steady-state versions of extended KdV equations, see the introduction for references. As precursors to the present work, however, the following special cases of (4.1) are of interest. For $\Gamma \equiv 0$, (4.1) was derived, and solved, to describe undular hydraulic jumps in turbulent flows that are fully developed far upstream (Grillhofer & Schneider 2003; Steinrück 2005). Generalizations to flows that are not fully developed far upstream of the undular jump have also been made, leading to $\Gamma = \text{const} \neq 0$ in (4.1) (Jurisits *et al.* 2007; Jurisits & Schneider 2012). Since hydraulic jumps, by definition, are associated with permanent changes of the surface elevation, undular-jump solutions do not satisfy the homogeneous boundary conditions (3.26).

For the special case $\beta = 0$, i.e. inviscid flow, the famous solitary-wave (soliton) solution satisfies both (4.1) and the boundary conditions (3.26). In the present notation it reads

$$H_1 = 3\text{sech}^2[(X - X_m)/2] \quad \text{for } \beta = 0, \tag{4.3}$$

where X_m is a free constant that locates the maximum surface elevation.

For turbulent flow, however, $\beta \neq 0$. Integrating (4.2*a*) and (4.2*b*), respectively, from $-\infty$ to $+\infty$, and observing the boundary conditions (3.26) together with (4.2*c*) gives the 'conservation' equations

$$\int_{-\infty}^{+\infty} (H_1 - \Gamma)\,\mathrm{d}X = 0, \tag{4.4a}$$

$$\int_{-\infty}^{+\infty} H_1(H_1 - \Gamma)\,\mathrm{d}X = 0. \tag{4.4b}$$

It follows from the integral conditions (4.4*a*) and (4.4*b*) that stationary solitary waves cannot persist in two-dimensional turbulent open-channel flow ($\beta \neq 0$) with a plane bottom of constant roughness ($\Gamma \equiv 0$). But, if the bottom roughness varies, i.e. $\Gamma = \Gamma(X)$, the situation is different. To begin with, the classical soliton solution $H_1^{(0)}$ according to (4.3) remains a solution of (4.1) also for $\beta \neq 0$ if $\Gamma(X) = H_1^{(0)}(X)$. But it is certainly not an easy task to produce the distribution of bottom roughness necessary to obtain that particular $\Gamma(X)$, e.g. in a laboratory experiment. Thus we admit more general roughness distributions and introduce an eigenvalue λ according to the relation

$$\Gamma(X) = \lambda\varphi(X), \tag{4.5}$$

with $\lambda = \text{const} = O(1)$ and $\varphi(X) = O(1)$. For (suitably) given $\varphi(X)$, the eigenvalue λ is then to be determined such as to permit a non-trivial solution of (4.1) subject to the boundary conditions (3.26). This nonlinear eigenvalue problem reflects the necessity to satisfy the condition of conservation of momentum flow, cf. appendix B.

Note that $\Gamma = O(1)$ implies $C^+ - C_r^+ = O(1)$, cf. (3.24). Since the friction coefficient, c_f, is of the order of $(\ln Re_\tau + \mathrm{C}^+ + \bar{C})^{-2} \ll 1$, cf. Schlichting & Gersten (2000), pp. 534–535, small changes of the reference value of the friction coefficient are sufficient for the appearance of a stationary solitary wave, provided the roughness distribution is in accord with the eigenvalue.

As an example that may be of relevance for laboratory experiments, a piecewise-constant bottom roughness is considered in what follows, i.e.

$$\varphi(X) \equiv 0 \quad \text{for } X < 0; \quad \varphi(X) \equiv 1 \quad \text{for } 0 < X < 1; \quad \varphi(X) \equiv 0 \quad \text{for } X > 1. \tag{4.6}$$

Equation (4.1) is to be solved subject to the boundary conditions (3.26), which implies an asymptotic decay of the form

$$H_1 \sim \exp(kX), \tag{4.7}$$

with $k < 0$ as $X \to \infty$ and $k > 0$ as $X \to -\infty$. Inserting into (4.1), with $\Gamma \equiv 0$ for $X \to \pm\infty$ as a consequence of (4.5) and (4.6), shows that k has to satisfy the cubic equation

$$k(k^2 - 1) = \beta. \tag{4.8}$$

For small values of β, (4.8) has the following roots that are in accord with the boundary conditions (3.26):

$$k_1 = -1 + \tfrac{1}{2}\beta + O(\beta^2); \quad k_2 = -\beta + O(\beta^2) \quad \text{for } X \to \infty; \tag{4.9a}$$

$$k_3 = +1 + \tfrac{1}{2}\beta + O(\beta^2) \quad \text{for } X \to -\infty. \tag{4.9b}$$

The asymptotic relation (4.7) with (4.9*a*) and (4.9*b*), respectively, will turn out to be useful for testing solutions for uniform validity, cf. § 4.2.

4.2. *Asymptotic solution for very weak dissipation*

Since β is assumed to be a small parameter, cf. (3.23), the limiting case $\beta \to 0$ is considered. Thus we write

$$H_1(X;\beta) = H_1^{(0)}(X) + \beta H_1^{(1)}(X) + \cdots; \quad \lambda(\beta) = \lambda^{(0)} + \beta\lambda^{(1)} + \cdots \quad \text{as } \beta \to 0, \tag{4.10}$$

to obtain from (4.1)

$$H_1^{(0)} = 3\operatorname{sech}^2[(X - X_m^{(0)})/2], \tag{4.11}$$

i.e. of course, the classical soliton solution, while the conservation equation (4.4*a*) gives

$$\lambda^{(0)} = \Phi^{-1} \int_{-\infty}^{+\infty} H_1^{(0)} \mathrm{d}X = 12/\Phi, \tag{4.12}$$

with

$$\Phi = \int_{-\infty}^{+\infty} \varphi \, \mathrm{d}X. \tag{4.13}$$

$X_m^{(0)}$ is a free constant that locates the maximum surface elevation in the limit $\beta \to 0$. It is to be determined from the second conservation equation, (4.4*b*), in the limit $\beta \to 0$, which gives the following condition:

$$\int_{-\infty}^{+\infty} [H_1^{(0)}]^2 \, \mathrm{d}X = \lambda^{(0)} \int_{-\infty}^{+\infty} H_1^{(0)} \varphi \, \mathrm{d}X. \tag{4.14}$$

For the case of piecewise-constant bottom roughness according to (4.6), one obtains from (4.12) with (4.13) the eigenvalue

$$\lambda^{(0)} = 12, \tag{4.15}$$

while (4.14) leads to the condition

$$\tanh\left[(1 - X_m^{(0)})/2\right] + \tanh(X_m^{(0)}/2) = 1/3. \tag{4.16}$$

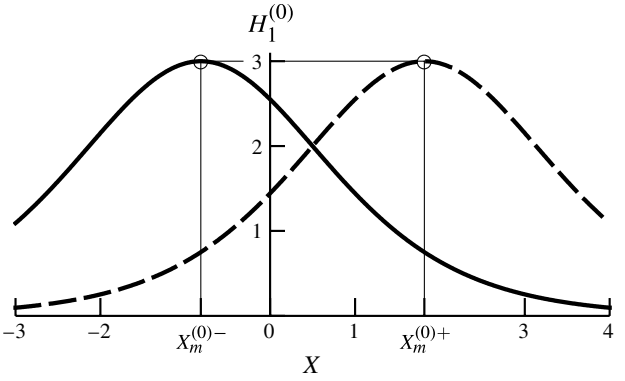

FIGURE 2. Surface elevation of the stationary solitary waves. Solid line: stable; broken line: unstable. The bottom roughness is enlarged in the region $0 < X < 1$.

Making use of well-known relationships for hyperbolic functions, the following dual solution of (4.16) can be found:

$$X_m^{(0)} = \tfrac{1}{2} \pm \operatorname{arcosh}(6\sinh\tfrac{1}{2} - \cosh\tfrac{1}{2}). \tag{4.17}$$

The numerical evaluation of (4.17) provides the two solutions

$$X_m^{(0)+} = +1.81635, \tag{4.18a}$$

$$X_m^{(0)-} = -0.81635. \tag{4.18b}$$

According to (4.18*a*) and (4.18*b*), respectively, the maximum surface elevation of the stationary solitary wave is located, in a first approximation, somewhat behind or, by the same amount, in front of the region of enlarged bottom roughness ($0 < X < 1$), see figure 2. Whether $X_m^{(0)+}$ and/or $X_m^{(0)-}$ belong to solutions that are stable, or unstable, will be investigated below (§ 5.2).

Expanding the first-order solution (4.11) for $X \to \pm\infty$ and comparing the result with the equations (4.7), (4.9*a*) and (4.9*b*), respectively, that describe the asymptotic behaviour of the full equation (4.1), it is easy to see that the first-order solution (4.11) is uniformly valid for $X \to \pm\infty$. However, it cannot be expected that the second-order terms in (4.10) will also be uniformly valid, the reason being that a formal expansion of the exponential function in (4.7) in terms of small values of the parameter β contains the secular term βX. To avoid the non-uniformity at the second order, one could introduce $\ln H_1$ as a new dependent variable and perform the asymptotic expansion for $\beta \to 0$ in terms of the new variable. That is beyond the scope of the present work, however. Since the second order will certainly require a numerical solution of the perturbation equation, it appears preferable to obtain, in future work, numerical solutions of the full equation (4.1) for arbitrary values of β.

5. Transient-flow solutions

5.1. *Evolution equation for slowly varying solitary waves*

There are well-established methods for treating slowly varying solitary waves on the basis of extended KdV equations. Thus (3.22) is transformed into the standard form of extended KdV equations by the transformation

$$X = \xi - \tau + X_0; \quad T = -\tau \quad (X_0 = \text{const}) \tag{5.1}$$

which gives

$$H_{1\xi\xi\xi} + H_1 H_{1\xi} + H_{1\tau} = \beta[H_1 - \Gamma(X)]. \tag{5.2}$$

For very small values of β, one may follow Scott (2003), p. 294, to obtain for a piecewise-constant roughness according to (4.5) and (4.6) the following solution in terms of the original coordinates:

$$H_1(X, T) = 3(1 - V)\mathrm{sech}^2\left[(X - X_0 - VT)\sqrt{1 - V}/2\right], \tag{5.3}$$

with the evolution equation

$$\frac{3}{\beta}\frac{\mathrm{d}V}{\mathrm{d}T} = 4(1 - V) - \lambda\left\{\tanh\left[(1 - X_0 - VT)\sqrt{1 - V}/2\right] + \tanh\left[(X_0 + VT)\sqrt{1 - V}/2\right]\right\} \tag{5.4}$$

for the slowly varying wave speed $V(T)$. According to (4.15), the eigenvalue λ can be replaced by $\lambda = \lambda^{(0)} = 12$. Note that the maximum surface elevation ('amplitude' of the solitary wave) is equal to $3(1 - V)$. Note also that the maximum surface elevation is located at $X_m = X_0 + VT$, i.e. at each moment the wave moves as if V were constant, with $X = X_0$ being the locus of the maximum surface elevation at time $T = 0$. For the special case $T \equiv 0$ see appendix C.

For $V \equiv 0$, (5.4) reduces to

$$\tanh[(1 - X_0)/2] + \tanh(X_0/2) = 1/3. \tag{5.5}$$

A comparison with (4.16) shows that $X_0 = X_m^{(0)}$, and (5.3) leads to the solution (4.11) for the stationary solitary wave, in accordance with the vanishing wave speed.

5.2. *Small perturbations of the stationary solitary waves*

Equation (4.16) has the two solutions $X_m^{(0)+}$ and $X_m^{(0)-}$, respectively, as given by (4.18*a*) and (4.18*b*). Assuming small perturbations of either one of the two stationary solitary waves due to a small initial velocity $V(0)$, with $|V(0)| \ll 1$, the evolution equation (5.4) may be linearized. Making use of (5.5) and integrating, one obtains

$$V = V(0)\exp[\beta(K_1 T + K_2 T^2)], \tag{5.6}$$

with

$$K_1 = -\tfrac{4}{3} + (1 - X_m^{(0)})\mathrm{sech}^2\left[(1 - X_m^{(0)})/2\right] + X_m^{(0)}\mathrm{sech}^2(X_m^{(0)}/2), \tag{5.7}$$

$$K_2 = \mathrm{sech}^2[(1 - X_m^{(0)})/2] - \mathrm{sech}^2(X_m^{(0)}/2). \tag{5.8}$$

With $X_m^{(0)}$ given by (4.17), the above constants become $K_1 = -1.153$ and $K_2 = \pm 0.369$. According to (5.6), K_2 characterizes the development of the perturbations for $T \gg 1$, as long as the perturbations remain small. For $X_m^{(0)} = X_m^{(0)+}$, $K_2 = K_2^+ = 0.369 > 0$, i.e. the wave speed grows beyond bounds with increasing time T, indicating that the stationary solitary wave with $X_m^{(0)} = X_m^{(0)+}$ is unstable. For $X_m^{(0)} = X_m^{(0)-}$, in contrast, $K_2 = K_2^- = -0.369 < 0$, i.e. the wave speed decays and, according to (5.3), the perturbed solitary wave returns to the stationary position.

The results may be understood on the basis of the following reasoning. Let us first consider the solution with $X_m^{(0)} = X_m^{(0)-} < 0$ according to (4.18*b*) and assume that the solitary wave is shifted slightly upstream due to a perturbation. Since, in this case, the maximum surface elevation is in front of the region of enlarged roughness,

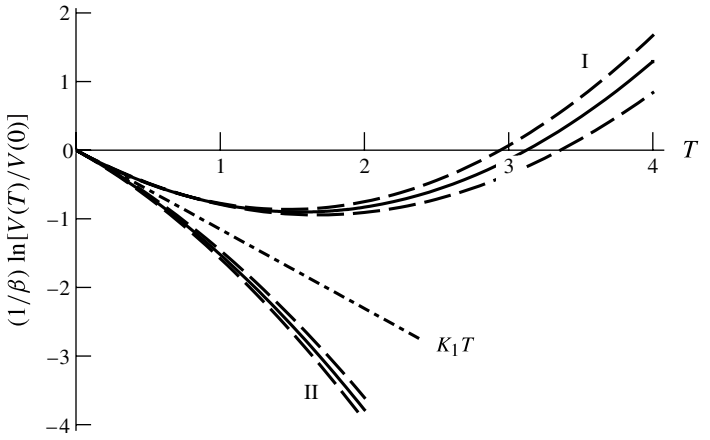

FIGURE 3. Comparison of numerical solutions of the evolution equation (5.4) ($\beta = 0.1$, dashed lines) with the analytical solution (5.6) (solid lines). Curves I are for $X_0 = X_m^{(0)+}$: solid line, $K_1T + K_2^+T^2$; upper dashed line, $V(0) = -\beta$; lower dashed line, $V(0) = +\beta$. Curves II are for $X_0 = X_m^{(0)-}$: solid line, $K_1T + K_2^-T^2$; upper dashed line, $V(0) = +\beta$; lower dashed line, $V(0) = -\beta$.

the perturbation leads to a reduction of the surface elevation and an increase of the flow velocity in the region of enlarged roughness. This increases dissipation, and the perturbed wave is swept downstream, i.e. back to the original position. If, on the other hand, the perturbation is a downstream shift, the opposite effect drives the wave back to the original position. However, in the case of the solution with $X_m^{(0)} = X_m^{(0)+} > 1$ according to (4.18*a*), similar reasoning leads to the conclusion that the perturbed wave is swept away from the original position.

5.3. *Initial value problems*

Equation (5.4), with $\lambda = 12$, can easily be solved numerically as an initial value problem for given values of $V(0)$. Once the wave speed, $V(T)$, is known, the wave amplitude, $H_{1m} = 3(1 - V)$, can easily be determined. Some results are given in figures 3–8.

Results for small perturbations of the stationary states that are characterized by $X_0 = X_m^{(0)+}$ or $X_0 = X_m^{(0)-}$ are given in figure 3. Numerical solutions of (5.4) are plotted in a way that allows good comparison with the analytical solution (5.6). The relatively large value $\beta = 0.1$ has been chosen for the dissipation parameter in order to make the differences between numerical and analytical results visible. For substantially smaller values of β, e.g. $\beta = 0.01$, the plots of the numerical and analytical results are practically indistinguishable.

Figures 4 and 5 show the development of the wave amplitude as a function of time, with β, which characterizes damping due to dissipation, as the parameter. The initial amplitude is the same in figures 4 and 5, i.e. equal to the amplitude of the stationary wave, but the initial position differs. For figure 4, the initial position of the wave is slightly downstream (upper half of the diagram), or slightly upstream (lower half of the diagram) of the position that is taken by the stable stationary wave. In both cases the wave approaches asymptotically the stable stationary state. The situation is different, of course, if the initial position of the wave is slightly downstream, or

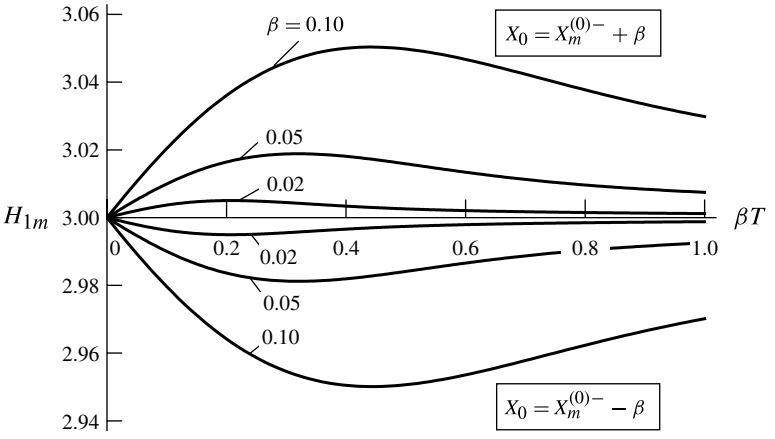

FIGURE 4. Wave amplitude H_{1m} versus slowly varying time βT, with β as parameter. Initial amplitude of waves: equal to amplitude of stationary solitary wave. Initial position of waves: $X_0 = X_m^{(0)-} + \beta$, i.e. slightly downstream (upper half of diagram), or $X_0 = X_m^{(0)-} - \beta$, i.e. slightly upstream (lower half of diagram), of stable stationary solitary wave.

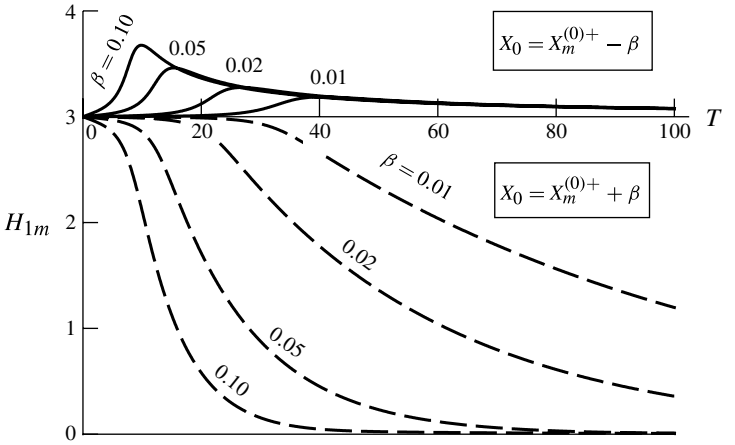

FIGURE 5. Wave amplitude H_{1m} versus time T, with β as parameter. Initial amplitude of waves: equal to amplitude of stationary solitary wave. Initial position of waves: $X_0 = X_m^{(0)+} - \beta$, i.e. slightly upstream (upper part of diagram), or $X_0 = X_m^{(0)+} + \beta$, i.e. slightly downstream (lower part of diagram), of unstable stationary solitary wave. Solid lines: waves approaching stable stationary solitary wave. Broken lines: decaying waves.

upstream, of the unstable stationary wave (figure 5). As can be expected from the results of the stability analysis presented above, the wave approaches asymptotically the stable stationary state in case of a small upstream shift, whereas the wave decays, while it is swept downstream, in case of a small downstream shift of the initial position.

For an initial position between the stable stationary wave and the unstable one, the transient behaviour of the wave is qualitatively the same as shown in figure 4 and in the upper part of figure 5, provided the initial wave amplitude is the same, i.e. that

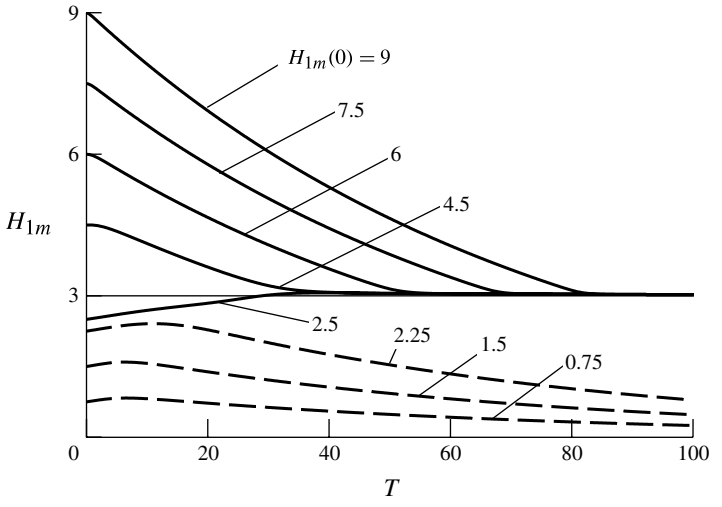

FIGURE 6. Wave amplitude H_{1m} versus time T, with initial amplitude $H_{1m}(0)$ as parameter. Damping parameter: $\beta = 0.01$. Initial position of maximum surface elevation: $X_0 = 0$. Solid lines: waves approaching stable stationary solitary wave. Broken lines: decaying waves.

of the stationary wave. That appears not surprising. But rather unexpected results are obtained when β and X_0 are fixed, but the initial amplitude is varied, see figure 6. For initial amplitudes that are larger, or only slightly smaller, than the amplitude of the stationary wave, the wave approaches asymptotically the stable stationary state according to the relation

$$H_{1m} = 3[1 + (X_0 - X_m^{(0)-})T^{-1} + O(T^{-2})] \quad \text{as } \beta T \to \infty, \tag{5.9}$$

which follows from (5.4) with (4.16) and $H_{1m} = 3(1 - V)$. However, if the initial amplitude is smaller than a critical value, which is approximately $H_{1m}(0)|_{crit} \approx 2.4676$ in the case of figure 6, the wave is swept downstream and decays.

Time versus space diagrams of the maximum surface elevation, H_{1m}, are given in figure 7 for selected values of initial amplitude, $H_{1m}(0)$, and initial position, X_0. Initial positions that are upstream of the stable stationary wave or downstream of the unstable stationary wave are included in figure 7. In both cases the wave approaches the stable stationary wave if the initial amplitude is sufficiently large, whereas the wave moves downstream, and decays, if the initial amplitude is too small to permit transition to the stable wave. The other cases shown in figure 7 are in qualitative accord with the results already discussed above.

Finally, figure 8 gives an idea of the shape of a wave that approaches the stable stationary wave, compared to a wave that decays slowly while it is swept downstream.

6. Conclusions and discussion

The extended KdV equation (3.22) that is obtained from an asymptotic analysis without recourse to turbulence modelling has eigensolutions that describe stationary solitary waves. The eigenvalue characterizes the piecewise-constant perturbation of the roughness of the channel bottom, while the eigenfunction gives the wave shape. The results show that the roughness enlargement required to support a stationary solitary wave is smaller for Froude numbers closer to the critical value 1. For small values

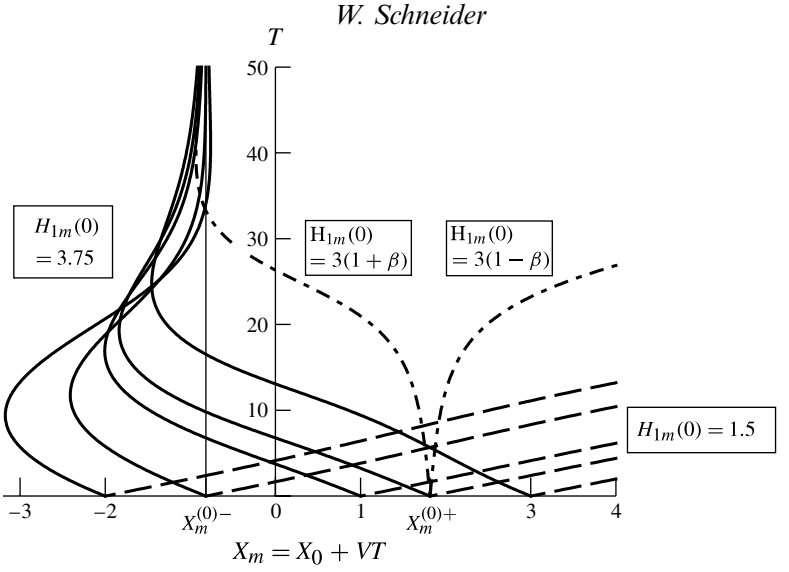

FIGURE 7. Locus of maximum surface elevation, $X_m = X_0 + VT$, as a function of time, T, for various initial loci $X = X_0$ at $T = 0$, i.e. $X_0 = \{-2, X_m^{(0)-}, 1, X_m^{(0)+}, 3\}$, with initial amplitude $H_{1m}(0)$ as parameter. Damping parameter: $\beta = 0.01$. Solid lines: $H_{1m}(0) = 3.75$, waves approach stable stationary solitary wave. Broken lines: $H_{1m}(0) = 1.5$, waves decay. Dashed-dotted lines: $H_{1m}(0) = 3(1 + \beta)$ and $H_{1m}(0) = 3(1 - \beta)$; the former waves approach the stable stationary solitary wave, the latter decay.

of a non-dimensional parameter β that characterizes dissipation, the eigenfunctions are, at first order, the classical solitary wave solutions for two different positions. The wave at the more downstream position turned out to be unstable with respect to small perturbations, whereas the other one represents the final state of a large class of transient solitary waves. Since these results are obtained on the basis of the assumption of slowly varying solitary waves, numerical investigations of the extended KdV equation are desirable, in particular concerning the possible appearance of shelves (cf. Knickerbocker & Newell 1980; Scott 2003), perhaps depending on the magnitude of the parameter β. Work is in progress to, hopefully, answer those questions. As in the case of the undular jump (Kalisch & Bjørkavåg 2010), an energy budget may also lead to interesting conclusions.

Experimental verification of the predictions is, of course, desirable. Available facilities, such as those used by Chanson & Montes (1995), Montes & Chanson (1998), Ohtsu *et al.* (2001), Ohtsu, Yasuda & Gotoh (2003), Gotoh, Yasuda & Ohtsu (2005) and Castro-Orgaz & Hager (2011) in their investigations on undular jumps, seem to be suitable. The value of β chosen for the examples shown in figures 5 to 7 is well within the reach of the facility used by Ohtsu *et al.* (2001, 2003) and Gotoh *et al.* (2005), and it is also in accord with the experiments reported by Lennon & Hill (2006). Experiments will have to take into account, however, that the predicted eigenvalue $\lambda^{(0)} = 12$ is only an approximation of the exact eigenvalue, as it is obtained from an asymptotic expansion of the extended KdV equation for small values of β, and, furthermore, the extended KdV equation itself is an approximation to the exact equations of motion.

Numerical solutions of the full equations of motion would also be of interest. For inviscid flow, numerical solutions of the Euler equations are available, cf. Dutykh & Clamond (2013). As far as turbulent flow is concerned, previous numerical

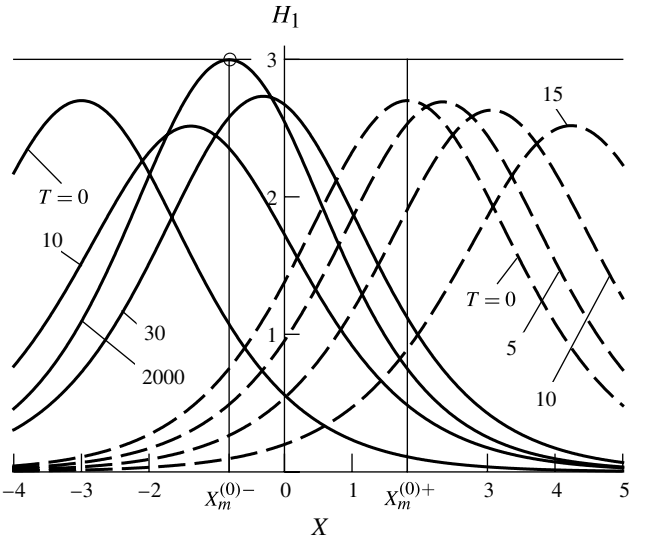

FIGURE 8. Surface elevations H_1 of slowly varying solitary waves at various times T. Damping parameter $\beta = 0.01$, initial amplitude $H_{1m}(0) = 2.7$. Solid lines: initial locus of maximum surface elevation $X_0 = -3$; solitary wave approaches stable stationary state. Broken lines: $X_0 = X_m^{(0)+} + \beta$; solitary wave moves downstream and decays slowly.

investigations of the related problem of the undular jump (Schneider *et al.* 2010) showed reasonable agreement between the asymptotic analysis and the numerical solution of the Reynolds-averaged equations of motion, irrespective of the turbulence model that was applied; see also the recent work by Rostami *et al.* (2012). More advanced numerical methods, e.g. large-eddy simulations of free-surface flows (Hassanzadeh, Sahin & Ozgoren 2012) could be helpful for evaluating the accuracy of less elaborate numerical investigations based on turbulence modelling.

Acknowledgements

The author is indebted to Mr C. Buchner, Dr R. Jurisits, Mr M. Müllner and Professor H. Steinrück for many fruitful discussions while this work was in progress. Mr Müllner also performed the numerical solutions of the evolution equation (5.4) and prepared the diagrams. Dr Jurisits' yet unpublished numerical solutions of the extended KdV equation helped the author to better understand the behaviour of the asymptotic solutions. In addition, Dr Jurisits drew the author's attention to references that were important for the analysis of the slowly varying solitary waves. Professor Steinrück and Dr Jurisits read a draft of the paper and made valuable comments that led to improvements of the presentation. Previous work is discussed in more detail following suggestions by referees, one of whom also provided valuable additional references. Finally, financial support by Androsch International Management Consulting GmbH is gratefully acknowledged.

Appendix A. Unsteady viscous wall layer

Since the continuity equation for incompressible flow does not contain a time derivative and, furthermore, the momentum equation for the lateral direction is of

lesser concern owing to the small thickness of the viscous wall (bottom) layer, it suffices to consider the momentum equation for the longitudinal direction to estimate the importance of terms containing time derivatives. Adding to (2.7*a*) the term that accounts for viscosity, one obtains

$$\delta Fr^2\left(\frac{3\varepsilon}{2}\frac{\partial\bar{U}}{\partial T}+\bar{U}\frac{\partial\bar{U}}{\partial X}+\bar{V}\frac{\partial\bar{U}}{\partial Y}\right)$$
$$=-\delta\frac{\partial\bar{P}}{\partial X}+\alpha-\alpha\left(\delta\frac{\partial\overline{U'^2}}{\partial X}+\frac{\partial\overline{U'V'}}{\partial Y}\right)+\frac{\sqrt{\alpha}Fr}{Re_\tau}\left(\delta^2\frac{\partial^2\overline{U}}{\partial X^2}+\frac{\partial^2\overline{U}}{\partial Y^2}\right). \quad \text{(A 1)}$$

Equation (A 1) is written in terms of the non-dimensional variables introduced in § 2 for the analysis of the defect layer. The viscous wall layer, however, is known to require a stretching of the variables as follows (Schlichting & Gersten 2000, pp. 570–572):

$$y^+=Re_\tau Y;\quad u^+=\bar{u}/u_{\tau r}=(Fr/\sqrt{\alpha})\bar{U};\quad v^+=\bar{v}/u_{\tau r}=(Fr/\sqrt{\alpha})\bar{V}. \quad \text{(A 2)}$$

From the continuity equation together with the boundary condition $\bar{V}=0$ at $Y=0$ it follows that $v^+\equiv 0$ in the limit of large Reynolds numbers. Introducing, then, the stretched variables into the momentum equation (A 1) and collecting the first-order terms on the left-hand side, gives the following equation:

$$\frac{\partial^2u^+}{\partial y^{+2}}-\frac{\partial\overline{U'V'}}{\partial y^+}=\frac{3\varepsilon\delta\mathrm{Fr}}{2\sqrt{\alpha}\,Re_\tau}\frac{\partial u^+}{\partial T}+\frac{\delta}{Re_\tau}u^+\frac{\partial u^+}{\partial X}-\frac{1}{Re_\tau}+\frac{\delta}{\alpha\,Re_\tau}\frac{\partial\bar{P}}{\partial X}+\cdots, \quad \text{(A 3)}$$

where the dots stand for higher-order terms. Using (2.1), the first coefficient on the right-hand side of (A 3) may be re-written as

$$\frac{3\varepsilon\delta}{2Re_\tau}\frac{\bar{u}_r}{u_{\tau r}}. \quad \text{(A 4)}$$

According to the well-known logarithmic friction law (Schlichting & Gersten 2000, p. 534), $\bar{u}_r/u_{\tau r}$ is of the order of $\ln Re_\tau$. As $\varepsilon\to 0$, $\delta\to 0$ and $Re_\tau\to\infty$, the time-derivative term on the right-hand side of (A 3) becomes negligible in comparison with the terms of order one on the left-hand side. This result justifies the application of matching conditions as if the flow in the viscous wall layer were steady, and in particular the use of the logarithmic overlap law.

Appendix B. Conservation of momentum flow rate

Steady flow is considered. Since the flow far upstream ($X\to-\infty$), as well as far downstream ($X\to+\infty$), is fully developed, the momentum flow rate far upstream is the same as far downstream, and the forces acting on the total volume of fluid must balance. The hydrostatic pressures far upstream and far downstream balance each other, and the forces that remain to be taken into account in the force balance are the following:

$$u_{\tau r}^2\int_{-\infty}^{+\infty}(U_\tau^2-1)\,\mathrm{d}X=g\alpha\bar{h}_r\int_{-\infty}^{+\infty}(H-1)\,\mathrm{d}X. \quad \text{(B 1)}$$

The coefficients in front of the integrals cancel according to (2.1), and introducing the expansions (2.4*a*) and (2.4*b*) gives, to the first order, the integral condition

$$\int_{-\infty}^{+\infty} [H_1 + (\overline{U'V'})_1(X, 0, T)]\,\mathrm{d}X = 0. \tag{B 2}$$

Substituting for $(\overline{U'V'})_1(X, 0, T)$ according to (3.16), and introducing Γ as defined in (3.24), one obtains (4.4*a*), i.e. the equation that determines the eigenvalue λ and, after expansion in terms of small values of β, the first-order eigenvalue $\lambda^{(0)}$.

Appendix C. Constant bottom roughness

If the roughness of the bottom is constant, the forcing term vanishes, i.e. $\Gamma \equiv 0$, and (5.2) reduces to the example considered by Scott (2003), p. 295, with reference to Ott & Sudan (1970) and Knickerbocker & Newell (1980). By definition, Scott's wave speed v is related to the present wave speed V as $v = 1 - V$, and his time t corresponds to $-T$ in the present notation. Two different signs cancel, and a solitary wave that is initially at rest in the present coordinate system, i.e. $V(0) = 0$, $v(0) = 1$, decays according to the relation

$$v = \exp(-4\beta T/3) \to 0 \quad \text{as } \beta T \to \infty. \tag{C 1}$$

The same result can be obtained by integrating (5.4) for the special case $\lambda = 0$, which corresponds to $\Gamma \equiv 0$ according to (4.5).

Note, however, that the analysis of the slowly varying solitary waves according to Scott (2003), p. 295, does not account for a shelf that may be generated behind the solitary wave, cf. Knickerbocker & Newell (1980) and Grimshaw *et al.* (2003). Regarding possible 'aging' of solitary waves, see Christov & Velarde (1995).

REFERENCES

ABD-EL-MALEK, M. B. & HELAL, M. M. 2011 Group method solutions of the generalized forms of Burgers, Burgers–KdV and KdV equations with time-dependent variable coefficients. *Acta Mech.* **221**, 281–286.

BINDER, B. J., VANDEN-BROEK, J.-M. & DIAS, F. 2005 Forced solitary waves and fronts past submerged obstacles. *Chaos* **15**, 037106.

BOSE, S. K., CASTRO-ORGAZ, O. & DEY, S. 2012 Free surface profiles of undular hydraulic jumps. *J. Hydraul. Engng* **138**, 362–366.

BROCCHINI, M. & PEREGRINE, D. H. 1998 The modelling of a spilling breaker: strong turbulence at a free surface. In *Proceedings of International Conference on Coastal Engng*, pp. 72–85. ASCE.

CAPUTO, J.-G. & STEPANYANTS, Y. A. 2003 Bore formation, evolution and disintegration into solitons in shallow inhomogeneous channels. *Nonlin. Process. Geophys.* **10**, 407–424.

CASTRO-ORGAZ, O. 2010 Weakly undular hydraulic jump: effects of friction. *J. Hydraul. Res.* **48**, 453–465.

CASTRO-ORGAZ, O. & CHANSON, H. 2011 Near-critical free-surface flows: real fluid flow analysis. *Environ. Fluid Mech.* **11**, 499–516.

CASTRO-ORGAZ, O. & HAGER, W. H. 2011 Observations on undular hydraulic jump in movable bed. *J. Hydraul. Res.* **49**, 689–692.

CHANSON, H. & MONTES, J. S. 1995 Characteristics of undular hydraulic jumps: experimental apparatus and flow patterns. *J. Hydraul. Engng* **121**, 129–144.

CHARDARD, F., DIAS, F., NGUYEN, H. Y. & VANDEN-BROECK, J.-M. 2011 Stability of some stationary solutions to the forced KdV equation with one or two bumps. *J. Engng Maths* **70**, 175–189.

CHRISTOV, C. I. & VELARDE, M. G. 1995 Dissipative solitons. *Physica* D **86**, 323–347.

DeKerf, F. 1988 Asymptotic analysis of a class of perturbed Korteweg-de Vries initial value problems. *CWI Tract 50*. Centre for Mathematics and Computer Science, Stichting Math. Centrum, Amsterdam.

Dias, F. & Vanden-Broeck, J.-M. 2002 Generalised critical free-surface flows. *J. Engng Maths* **42**, 291–301.

Dias, F. & Vanden-Broeck, J.-M. 2004 Trapped waves between submerged obstacles. *J. Fluid Mech.* **509**, 93–102.

Dutykh, D. 2009 Visco-potential free-surface flows and long wave modelling. *Eur. J. Mech. (*B*/Fluids*) **28**, 430–443.

Dutykh, D. & Clamond, D. 2013 Efficient computation of steady solitary gravity waves (submitted).

Dutykh, D. & Dias, F. 2007 Viscous potential free-surface flows in a fluid layer of finite depth. *C. R. Acad. Sci. Paris* I **345**, 113–118.

El, G. A., Grimshaw, R. H. J. & Kamchatkov, A. M. 2007 Evolution of solitary waves and undular bores in shallow-water flows over a gradual slope with bottom friction. *J. Fluid Mech.* **585**, 213–244.

Gersten, K. & Herwig, H. 1992 *Strömungsmechanik. Grundlagen der Impuls-, Wärme- und Stoffübertragung aus asymptotischer Sicht*. Vieweg.

Gotoh, H., Yasuda, Y. & Ohtsu, I. 2005 Effect of Channel Slope on Flow Characteristics of Undular Hydraulic Jumps. In *River Basin Management III* (ed. C.A. Brebbia & J.S.A. do Carmo), WIT Transactions on Ecology and the Environment, pp. 33–42. WIT Press.

Grillhofer, W. 2002 Der wellige Wassersprung in einer turbulenten Kanalströmung mit freier Oberfläche. Dissertation, Technische Universität Wien, Vienna, Austria.

Grillhofer, W. & Schneider, W. 2003 The undular hydraulic jump in turbulent open channel flow at large Reynolds numbers. *Phys. Fluids* **15**, 730–735.

Grimshaw, R. 2005 Korteweg-de Vries equation. In *Nonlinear Waves in Fluids: Recent Advances and Modern Applications* (ed. R. Grimshaw). CISM Courses and Lectures, vol. 483, pp. 1–28. Springer.

Grimshaw, R. 2007 Internal solitary waves in a variable medium. *GAMM-Mitt.* **30/1**, 96–109.

Grimshaw, R. 2010 Exponential asymptotics and generalized solitary waves. In *Asymptotic Methods in Fluid Mechanics: Survey and Recent Advances* (ed. H. Steinrück). CISM Courses and Lectures, vol. 523, pp. 71–120. Springer.

Grimshaw, R., Pelinovsky, E. & Talipova, T. 2003 Damping of large-amplitude solitary waves. *Wave Motion* **37**, 351–364.

Grimshaw, R. H. J., Zhang, D.-H. & Chow, K. W. 2007 Generation of solitary waves by transcritical flow over a step. *J. Fluid Mech.* **587**, 235–254.

Hager, W. H. & Hutter, K. 1984 On pseudo-uniform flow in open channel hydraulics. *Acta Mech.* **53**, 183–200.

Handler, R. A., Swean, T. F. Jr., Leighton, R. I. & Swearingen, J. D. 1993 Length scales and the energy balance for turbulence near a free surface. *AIAA J.* **31**, 1998–2007.

Hassanzadeh, R., Sahin, B. & Ozgoren, M. 2012 Large eddy simulation of free-surface effects on the wake structures downstream of a spherical body. *Ocean Engng* **54**, 213–222.

Johnson, R. S. 1972 Shallow water waves on a viscous fluid – the undular bore. *Phys. Fluids* **15**, 1693–1699.

Johnson, R. S. 1997 *A Modern Introduction to the Mathematical Theory of Water Waves*. Cambridge University Press.

Jurisits, R. & Schneider, W. 2012 Undular hydraulic jumps arising in non-developed turbulent flows. *Acta Mech.* **223**, 1723–1738.

Jurisits, R., Schneider, W. & Bae, Y. S. 2007 A multiple-scales solution of the undular hydraulic jump problem. In *Proc. Appl. Math. Mech. (PAMM)* **7**, 4120007-4120008/.

Kalisch, H. & Bjørkavåg, M. 2010 Energy budget in a dispersive model for undular bores. *Proc. Estonian Acad. Sci.* **59**, 172–181.

Kang, T. H. 2009 The undular tidal bore in turbulent free-surface flow at large Reynolds number (in Korean). Master thesis, Changwon National University, Changwon, Korea in cooperation with Vienna University of Technology, Vienna, Austria.

KLUWICK, A. (Ed.) 1998 *Recent Advances in Boundary Layer Theory*. CISM Courses and Lectures, vol. 390. Springer.

KLUWICK, A., COX, E. A., EXNER, A. & GRINSCHGL, C. 2010 On the internal structure of weakly nonlinear bores in laminar high Reynolds number flow. *Acta Mech.* **210**, 135–157.

KNICKERBOCKER, C. J. & NEWELL, A. C. 1980 Shelves and the Korteweg-de Vries equation. *J. Fluid Mech.* **98**, 803–818.

KOMORI, S., NAGAOSA, R., MURAKAMI, Y., CHIBA, S., ISHII, K. & KUWAHARA, K. 1993 Direct numerical simulation of three-dimensional open-channel flow with zero-shear gas–liquid interface. *Phys. Fluids* A **5**, 115–125.

LEIBOVICH, S. & RANDALL, J. D. 1971 Dissipative effects on nonlinear waves in rotating fluids. *Phys. Fluids* **14**, 2559–2561.

LEIBOVICH, S. & RANDALL, J. D. 1973 Amplification and decay of long nonlinear waves. *J. Fluid Mech.* **53**, 481–493.

LENNON, J. M. & HILL, D. F. 2006 Particle image velocity measurements of undular and hydraulic jumps. *ASCE J. Hydraul. Engng* **132**, 1283–1294.

MONTES, J. S. & CHANSON, H. 1998 Characteristics of undular hydraulic jumps: experiments and analysis. *ASCE J. Hydraul. Engng* **124**, 192–205.

MILES, J. W. 1983*a* Solitary wave evolution over a gradual slope with turbulent friction. *J. Phys. Oceanogr.* **13**, 551–553.

MILES, J. W. 1983*b* Wave evolution over a gradual slope with turbulent friction. *J. Fluid Mech.* **133**, 207–216.

MOHAMED, A. N. 2010 Modelling of free jumps downstream symmetric and asymmetric expansions: theoretical analysis and method of stochastic gradient boosting. *J. Hydrodyn.* **22**, 110–120.

NEWELL, A. C. 1985 *Solitons in Mathematics and Physics*. Society for Industrial and Applied Mathematics.

NEZU, I. & RODI, W. 1986 Open-channel flow measurements with a laser Doppler anemometer. *ASCE J. Hydraul. Engng* **112**, 335–355.

OHTSU, I., YASUDA, Y., GOTOH, H. & IAHR, M. 2001 Hydraulic condition for undular-jump formations. *J. Hydraul. Res.* **39**, 203–209.

OHTSU, I., YASUDA, Y. & GOTOH, H. 2003 Flow conditions of undular hydraulic jumps in horizontal rectangular channels. *J. Hydraul. Engng* **129**, 948–955.

OTT, E. & SUDAN, R. N. 1970 Damping of solitary waves. *Phys. Fluids* **13**, 1432–1434.

PELINOVSKY, E. N., STEPANYANTS, YU. & TALIPOVA, T. 1993 Nonlinear dispersion model of sea waves in the coastal zone. *J. Korean Soc. Coast. Ocean Engrs* **5**, 307–317.

RODI, W. 1993 *Turbulence Models and their Application in Hydraulics*, 3rd edn. Balkema.

ROSTAMI, F., YAZDI, S. R. S., SAID, M. A. M. & SHAROKHI, M. 2012 Numerical simulation of undular jumps on graveled bed using volume of fluid method. *Water Sci. Technol.* **66.5**, 909–917.

SCHLICHTING, H. & GERSTEN, K. 2000 *Boundary Layer Theory*, 8th edn. Springer.

SCHNEIDER, W. 2005 Near-critical free-surface flows. In *Proceedings of 2nd Shanghai International Symp. Nonlinear Science and Applications (Shanghai NSA'05)*, Section 8.6 *Free and Moving Boundary Problems*.

SCHNEIDER, W., JURISITS, R. & BAE, Y. S. 2010 An asymptotic iteration method for the numerical analysis of near-critical free-surface flows. *Intl J. Heat Fluid Flow* **31**, 1119–1124.

SCOTT, A. 2003 *Nonlinear Science*, 2nd edn. Oxford University Press.

STEINRÜCK, H. 2005 Multiple scales analysis of the steady-state Korteweg-de Vries equation perturbed by a damping term. *Z. Angew. Math. Mech.* **85**, 114–121.

STEINRÜCK, H. 2010 Multiple scales analysis of the turbulent undular hydraulic jump. In *Asymptotic Methods in Fluid Mechanics: Survey and Recent Advances* (ed. H. Steinrück). CISM Courses and Lectures, vol. 523, pp. 197–219. Springer.

STEINRÜCK, H., SCHNEIDER, W. & GRILLHOFER, W. 2003 A multiple scales analysis of the undular hydraulic jump in turbulent open channel flow. *Fluid Dyn. Res.* **33**, 41–55.

SVENDSEN, I. A., VEERAMONY, J., BAKUNIN, J. & KIRBY, J. T. 2000 The flow in weak turbulent hydraulic jumps. *J. Fluid Mech.* **418**, 25–57.

VAN DYKE, M. 1975 *Perturbation Methods in Fluid Mechanics*, annotated edn. Parabolic.

WHITHAM, G. B. 1999 *Linear and Nonlinear Waves*. Wiley.